

1. Non-destructive and contactless objective quality evaluation on table grapes
2. Automatic feature selection and configuration in a Computer Vision System
3. Automatic feature selection outperformed human selection
4. Classification by Random Forest provided 100 % accuracy on cv Italia and 92% on cv Victoria

29 **Abstract**

30 Quality rating is currently accomplished by non-destructive and subjective sensory evaluation or by
31 objective and destructive analytical techniques. There is a strong need of an objective non-destructive
32 contactless quality evaluation system to monitor **fruit and vegetable** along the whole supply chain.
33 This paper proposes a Computer vision system to satisfy this request. Image processing and machine
34 learning techniques have been combined to develop a Computer vision system whose configuration
35 and tuning has been strongly simplified: that makes easier its deployment in real applications. The
36 system has been verified **on two table grape cultivars (Italia and Victoria)** against three different
37 classification tasks. **The first considered five quality levels (5, 4, 3, 2, 1); the second separated the**
38 **higher fully marketable quality levels (5 and 4) from the boundary (3) and the waste (2 and 1); the**
39 **third separated the higher fully marketable quality levels (5 and 4) from the other three (3, 2 and 1).**
40 The system achieved a cross-validation classification accuracy up to 92% on the cultivar Victoria and
41 up to 100% on the cultivar Italia. The obtained results support its capability of powerfully, flexibly
42 and continuously monitoring the quality of the complete production along the whole supply chain.

43 **Keywords:** table grapes; quality evaluation; Computer vision system; random forest classifier.

44 **1. Introduction**

45 Table grape (*Vitis vinifera* L.) is a non-climacteric fruit subject to serious quality loss after harvest,
46 mainly due to water loss, which cause stem browning and sensitivity to microbial decay. Rachis
47 browning is the most important physiological disorder of table grapes post-storage, while the primary
48 pathological spoilage problem is decay caused by *Botrytis cinerea* (Lichter, 2016).

49 **Colour characteristics, firmness (skin, pulp and whole berry), chemical and volatile composition are**
50 **the main sensory attributes evaluated by consumers.** Usually, a green rachis is an indicator of
51 freshness and hence a brown rachis can be a cause of consumer rejection and fruit waste. Generally,
52 the quality level of table grape is determined through sensory and subjective determination combined
53 to analytical and destructive techniques, which are time consuming and sometimes may require

sophisticated equipment. Research has been focused on developing non-contact, rapid, environmental-friendly and accurate methods for non-invasive evaluation of quality in fruits and vegetables (Liu et al., 2017). Among these, Computer vision systems (CVSs) may be applied to extend quality prediction and discrimination along the whole supply chain from harvesting up to consumers. CVS combines mechanics, optical instrumentation, electromagnetic sensing and digital image processing technology (Patel et al., 2012). Computer vision systems are widely used to accomplish quality control on fruit and vegetables (Blasco et al., 2017). As reported by many Authors, CVS was used to assess quality and marketability of tomatoes (Arias et al., 2000), artichokes (Amodio et al., 2011), fresh-cut nectarines (Pace et al., 2011), fresh-cut lettuce (Pace et al., 2014), fresh-cut radicchio (Pace et al., 2015) and rocket leaves (Cavallo et al., 2017). Moreover, assessment of solid soluble content of table grape was also conducted using the hyperspectral imaging systems with the scatter mode by Baiano et al. (2012). In addition, Bahar (2017) evaluated quality of table grape measuring rachis browning through no destructive image analysis. ~~Colour, with shape and size, represents a strong index of product quality for both producers and consumers and is therefore used by humans or by instruments to monitor the quality. Computer vision systems have been used also to evaluate the quality of grapes.~~ Pothen et al., (2016) proposed a vision-based system to evaluate the ripeness of grapes with the aim to monitor the temporal evolution of vineyard and the spatial map of fruits to support the decision about harvest dates and locations. The system uses the H component of the Hue Saturation Value (HSV) colour space to be independent on spectrally uniform illumination change. The thresholds on the H information that separate the considered classes of ripeness are set empirically by the designers of the system. Unfortunately, the illumination often changes in its spectral distribution both indoor and outdoor: it is therefore generally better to check the constancy of colour measures and to correct them whenever needed as the proposed system does using a colour reference in the scene. Rodriguez-Pulido et al., (2012) used image analysis to evaluate the maturation of grapes and the cultivar by analyzing the seeds and the berries. A colour-chart and a carefully controlled set-up are used to make consistent the acquisition process and manually set thresholds are used to separate the classes of interest. Raban et al. (2013) developed a statistical method of image

81 analysis to measure rachis browning in four table grape cultivars in growth or storage. In Rahman and
82 Hellicar, 2014, a classification of mature grape bunches was shown. Their work consists of a
83 segmentation step to detect circles (berries) in the scene, RGB and HSV colour features extraction and
84 SVM classifiers training to predict mature grape bunches and undeveloped grape bunches. Nogales-
85 Bueno et al. (2014) presented a hyper-spectral imaging system to predict, on grape skin, total phenolic
86 concentration, sugar concentration, titratable acidity and pH using Modified Partial Least Squared
87 Regression (MPLS). Diago et al. (2015) developed an image analysis system to predict yield
88 components (berry weight, number of berries per cluster and cluster weights) by means of contour
89 extraction and circle detection. These predicted variables are key components and have an impact on
90 cluster architecture and compactness. Aquino et al., (2018a) use image analysis, on an android-
91 smartphone platform, to assess the number of berries in grapevine bunches at a phenological stage
92 between berry-set and cluster-closure. Their system requires a dark background box to be placed
93 behind the cluster to isolate the cluster, to enhance its separation from the background and to prevent
94 mutual reflections between adjacent bunches. The RGB image are converted to the CIELAB colour
95 space before any processing. Maximum light reflection points and morphological processing identify
96 and select potential berries. False positives are discarded by a neural network trained on a proper set
97 of berry descriptors. Mean and standard deviation of the a and b components in the CIELAB colour
98 space are used as colour descriptors. Moving the CVS on a portable hardware platform such as a
99 smartphone certainly extends its applicability along the supply chain but require further efforts to
100 solve all the problems related to weaker constraints on the acquisition set-up (background, geometry
101 and lighting). In Aquino et al. (2018b) a non-invasive and in-field yield prediction was presented. This
102 research involves several stages as input images pre-processing, identification of berry candidates and
103 neural network training in yield components prediction. Sollazzo et al., (2018) have verified the
104 correlation between colour and chemical compound related to the assessment of grapes ripeness using
105 colour measures obtained by a colorimeter or subjectively evaluated using a properly designed colour
106 chart. On the other hand, our system has been designed to reduce the manual interventions in both
107 configuration and tuning of the algorithms to enhance the performance and to simplify its application

108 to different products. The aim of the proposed system is to achieve contactless and no destructive
109 quality evaluation of table grape during cold storage using a colour reference in the scene: the system
110 fully exploits image analysis and machine learning techniques to reduce human intervention in
111 configuration and tuning to the minimum. This significantly simplifies its deployment and application
112 in several points of the supply chain extending the quality monitoring and improving the product
113 management.

114

115 **2. Materials and Methods**

116 *2.1. Plant material and experimental setup*

117 Table grapes (*Vitis vinifera* L., cvs *Italia* and *Victoria*) were provided by a farm (Ermes snc,
118 Noicattaro, Bari, Italy) in two harvests (September and October) at the same maturity stage (total
119 soluble solid content of 16° Brix, according to OIV, 2008) and were transported within 1 h from
120 harvest to the Postharvest laboratory. One hundred bunches for each cultivar were placed in open
121 polypropylene bags (25 × 30 cm, 30 µm, Carton Pack, Rutigliano, Italy), each one containing 1 bunch
122 (about 1kg of product) and stored at two different temperatures (5 and 10 °C) for 25 and 20 days
123 respectively for cv *Victoria* and 37 and 27 days respectively for cv *Italia*. The length of storage was
124 defined as the number of days needed to reach the lowest quality level (QL) at each temperature.
125 Thus, during storage, for each cultivar and storage temperature, 10 table grape bunches were
126 evaluated by 8 panellist, in order to assign a QL using the following subjective scale: 5 = very good
127 (rachis green, firm berries, no signs of decay), 4 = good (rachis green with slight symptom of
128 dehydration, firm berries), 3 = limit of acceptability or marketability (rachis moderately browned, firm
129 berries slightly brown), 2 = poor (evident signs of browning of rachis, loss of firmness of berries), and
130 1 = very poor (unacceptable quality due to decay). Thus, 100 bunches of *Italia* and 100 bunches of
131 *Victoria* were used for the QL assessment. The QL3 was considered the minimum threshold of
132 acceptance for sale or consumption (Cefola et al. 2018), therefore values below 3 indicated a waste
133 product (Figure 1).

134 2.2. *Workflow of the proposed approach to predict the quality level of table grape bunches*

135 The proposed approach to contactless and non-destructive evaluation of quality of table grapes by a
136 Computer **vision system** (CVS) involves different tasks: acquisition of a dataset of calibrated colour
137 images annotated with the **QL** of the corresponding table grape; proper pre-processing of the acquired
138 images; colour features identification and extraction; training, tuning and testing a Random Forest
139 Classifier (RFC). This workflow is graphically represented in Figure 2.

140

141 2.2.1. *Data acquisition and pre-processing*

142 Calibrated colour images were acquired and processed for each cultivar (**Italia and Victoria**); **in total,**
143 **for each cultivar, the data set was composed by 400 images, obtained acquiring each bunch 4 times in**
144 **different position.** Images (for each QL from 5 to 1) were acquired using the set-up previously
145 reported (Cavallo et al., 2017 and, 2018; Pace et al., 2015 and 2017) using a 3CCD (Charged
146 Coupled Device) digital camera (JAI CV-M9GE) with a dedicated CCD for each colour channel. The
147 optical axis of the Linos MeVis 12 mm lens system was perpendicular to the black background. Eight
148 halogen lamps (divided along two rows placed at the two sides of the imaged area) were oriented at a
149 45° angle with respect to the optical axis. The images were saved using the uncompressed TIFF
150 format. A small X-Rite colour-chart with 24 patches was placed into the scene to estimate colour
151 variations due to environmental conditions and sensor characteristics by comparing the expected
152 numerical values released by X-Rite with the measured ones. The colour-chart was automatically
153 detected regardless its position and orientation. Its white patch was used to white-balance the image: **a**
154 **correction coefficient was evaluated (dividing the reference value by the measured value) and**
155 **multiplied to each band to reduce the distance between the measured white and the reference one.**
156 **Noisy pixels, for which at least one channel was greater than the maximum allowed value in the**
157 **colour space (i.e. 255) after the white balance, were removed.** The CVS automatically separated the
158 product at hand (foreground) from the background using two thresholds automatically derived from
159 the analysis of the whole image in the HSV colour space, without any human intervention. **The**

160 segmentation was used only to identify the region belonging to the product (to be further processed)
161 and not to separate different parts of the table grape. The segmentation approach was conservative:
162 thresholds were derived to discard all the background pixels even at the cost of removing some
163 peripheral parts at the borders of the product.

164

165 2.2.2. Feature extraction

166 From every calibrated image related to each QL and cultivar suitable features were extracted.
167 Specifically, two set of features were used: the first one was represented by statistical measures
168 evaluated over the whole foreground on the channels in the CIELAB colour space (Cavallo et al.,
169 2017); the second one was derived by a centroid-based colour segmentation algorithm (Pace et al.,
170 2015).

171 To evaluate the first set of features all the pixel belonging to the foreground were converted from the
172 device dependent RGB space into the device independent CIELAB colour space in which the L^*
173 channel expresses the lightness dimension (in the range $[0,100]$) while a^* and b^* represent
174 respectively the green-red and blue-yellow colour components (both in the range $[-127,128]$). Mean
175 and standard deviation (std) of each colour channel (L^* , a^* and b^*) were computed. Moreover,
176 $\text{mean}(a^*) \cdot \text{mean}(b^*)$, $\text{mean}(L^*) \cdot \text{mean}(a^*)$, $\text{mean}(L^*) \cdot \text{mean}(b^*)$, $\text{mean}(a^*)/\text{mean}(b^*)$,
177 $\text{mean}(a^*)/\text{mean}(L^*)$ and $\text{mean}(b^*)/\text{mean}(L^*)$ were considered. All these features were normalized using
178 the min-max method to balance their influence on the final results: the obtained 12 normalized
179 features were all positive and in the range $[0,1]$.

180 To automatically obtain the second set of features, a hierarchical clustering algorithm was applied to
181 the calibrated colour images. This unsupervised machine learning algorithm yields a structure called
182 dendrogram that hierarchically groups all the colours according to a chosen distance metric. This
183 structure can be cut at different depth providing, at the k^{th} level, k clusters. The Euclidean distance
184 was used as distance metric and the dendrogram was cut at the 2nd level providing two clusters. Two
185 centroids were identified to represent these two clusters: they were therefore used to segment each
186 image into two different regions. Specifically, all pixels belonging to the foreground were converted

187 into CIELAB space and assigned to the nearest identified centroid using Euclidean distance (colour
188 segmentation). Finally, the two percentages p_1 and p_2 of pixels belonging to the two clusters were
189 used as further features to describe colour changes of the product surface due to senescence. In Figure
190 3 is shown an example of centroid-based image segmentation carried out on table grapes labelled as
191 QL5 and QL1. The image shows the difference between the two quality levels in terms of percentages
192 of pixels belonging to the two relevant colours: it is important to note that even if they are roughly
193 associated to green and brown they are chosen freely and automatically by the system to represent the
194 colorimetric characteristics of the product at hand and are not constrained to mimic what humans
195 consider to be relevant for the desired task. Statistical features and percentages produce a vector
196 with 14 basic elements. Moreover, additional polynomial features were composed by combining
197 these basic features to further improve the expressivity of the feature vector. Nonlinear functions are
198 often very difficult to fit and polynomial features can improve models' accuracies. Anyway, high
199 polynomial degrees should be avoided to prevent undesirable effects (overfitting, curse of
200 dimensionality). A proper combination of polynomial features and tuning of their degree must be
201 found to maximize effectiveness.

202

203 2.2.3. Random Forest models

204 Random Forest has been chosen as the supervised classification model to predict the QL of table
205 grapes. This ensemble model is composed by multiple predictive trees whose combination achieves a
206 predictive performance greater than each single component. Specifically, Random Forest, also called
207 decision forest, consists of an ensemble of decision trees with feature and sample bagging: each tree is
208 built on a sample (bootstrap) of the training set using a random feature subset instead of the whole
209 feature space. This technique entails two main advantages: (i) in spite of a slight bias growth, variance
210 (overfitting) is drastically reduced and (ii) the predictive performance (obtained by averaging the
211 answers of the different trees) is generally improved.

212 Since the target variable (QL) is a discrete variable that can assume five possible values (from QL5 to
213 QL1) each decision tree is a classification tree. Nonetheless an equivalent regression ensemble model

214 could be used with numerical response variables using regression trees as shown in Cavallo et al.
215 (2017). Two cross-validation schemes were nested to implement this model. An external 5-fold cross-
216 validation was applied to the available samples (and to their associated feature vectors) to evaluate the
217 predictive performance of the complete Random Forest model; an internal 10-fold randomized search
218 was exploited to find the best configuration of the parameters (model tuning) at each iteration of the
219 external cross-validation scheme.

220 To evaluate the efficacy of the automatic feature selection approach, each run was repeated working
221 also on a set of manually selected features. Specifically, on the base of the visualization of bivariate
222 graphics showing the relationship between predictors and target, three features (“mean of a^* ”, “mean
223 of b^* ” and centroid-based colour percentage) were chosen. The comparison of performances obtained
224 using these two different sets of features was used to assess the effectiveness of the automatic feature
225 selection.

226 Furthermore, three different resolution of classification of QL were checked. QL5 and QL4 represent
227 the higher fully marketable qualities, QL3 represents the limit of acceptability or marketability while
228 QL2 and QL1 represent only wastes. Therefore, the following classification tasks were verified:

- 229 a) 5 classes classification: QL5 vs QL4 vs QL3 vs QL2 vs QL1;
- 230 b) 3 classes classification: {QL5, QL4} vs QL3 vs {QL2, QL1};
- 231 c) 2 classes classification: {QL5, QL4} vs {QL3, QL2, QL1}.

232 The task a is the most informative but proved to be slightly less robust. The task c is the less detailed
233 but was much more robust and can timely alert about the achievement of the limit of acceptability or
234 marketability: this can activate special marketing policy or can send the product toward alternative
235 recycling paths to reduce waste. Two different approaches were compared during the modelling
236 phase: in one of them features were manually selected before running the machine learning pipeline;
237 in the other case features were automatically identified by the learning algorithm. Some of the
238 parameters of the Random Forest classifier were manually set while other were optimized during the
239 model tuning using an inner cross-validation randomized search. The following parameters were
240 manually set: the gini-index (used to measure the quality of splits), the square root of the number of

241 total features (adopted as the maximum number of features for each classification tree), the minimum
242 number of samples required to split an internal node (set to the value 2), the minimum number of
243 samples required for a leaf node (set to 1). Bootstrap samples was used (in addition to bootstrap
244 features): that is samples were drawn with replacement. The generalization accuracy was estimated by
245 using out-of-bag (oob) score: this method avoids the need of a separate test set by considering, for
246 each training instance i , the average error made by classifying using only the trees of the random
247 forest that do not contain the instance i in their bootstrap samples. The following parameters were
248 optimized by model tuning: number of trees (in the range [25,50]), maximum depth of trees (in the
249 range [5,10]) and degree of polynomial features (in the range of [2,6]). Because tuning parameters
250 requires a validation set, a nested cross-validation was used: the internal cross-validation used for
251 tuning split the training data used by the outer cross-validation.

252 **3.0. Results and Discussion**

253 To manually select the features by evaluating the relationship between target and predictors, features
254 were visualized using bivariate plots. A strong correlation was observed between centroid-based
255 percentage features p_1 and p_2 and QLs of the cultivar **Italia**. It was possible to separate higher QLs
256 table grapes belonging to QL5 and QL4 from QL3, QL2 and QL1 ~~remaining grapes~~. This interesting
257 relationship is shown in **Figure 4**. Similarly, a good correlation was observed between channel
258 features (mean of L^* , a^* and b^*) and **table** grapes QLs.

259 The performances of the predictive models were measured using classification accuracy (correct
260 predictions/total predictions) averaged over the results of the outer 5-fold cross-validation. In fact,
261 model tuning was performed by an inner 10-fold cross-validation, while outer 5-fold cross-validation
262 was used only to evaluate learned models. Each fold was composed by stratified sampling to
263 guarantee that each QL was properly represented in each fold. The same pipeline was repeated twice:
264 one with manually chosen features and one with automatic selected features.

265 In Table 1 predictive performances for the three different classification tasks between manual feature
266 selection and automatic feature selection are compared on both the cultivars Italia and Victoria. The

267 performance on the cultivar Italia was better than the one on cultivar Victoria. Probably this is related
268 to the fact that in cv Italia, the loss of quality is mainly due to the colour change of berries, while in
269 Victoria this is less discriminant and needs to be integrated by other quality traits (such as berry
270 dehydration, rachis browning and desiccation) to characterize the QLs.

271 The separation of all the five classes can be achieved with lower robustness. On the other hand, to
272 separate the two first QLs (5 and 4) is not relevant in real applications. Even the separation of the last
273 two QLs (2 and 1) is often not significant because they both correspond to products that cannot be
274 sold anymore. Along the supply chain is generally important to detect the achievement of QL3
275 because it represents the limit of marketability (Amodio et al., 2007). The system has been able to
276 separate the highest QLs (5 and 4) from the other (from QL3 to QL1) with an accuracy of 100 % on
277 cultivar Italia and of 92% on cultivar Victoria. Similarly, the same CVS, applied to fresh-cut lettuce,
278 resulted able to discriminate the acceptable product (ranging from QL5 to QL3) from the waste (QL
279 =2 or 1), starting from features based on colour parameters and also to provide an accurate estimate of
280 the ammonium content, giving a non-destructive evaluation of a chemical and objective parameter
281 (Pace et al., 2014).

282 The experiments showed that the automatic feature selection was able to outperform the manually
283 selected features. The ensemble model achieved better scores regardless the cultivar or the specific
284 classification tasks. This is important because the configuration of the system can be done
285 automatically by feeding in the system a quite large set of potential features, leaving to machine
286 learning tools the task of selecting how many and which characteristics are better suited to achieve the
287 classification task at hand. This makes the extension of the system to other products or cultivar much
288 easier and achievable even by non-expert users. The proposed models are based on a complex
289 combination of factors extracted from digital images which allow to predict the sensory quality with
290 good performance. This overcomes the limits of linear models (Baiano et al; 2012) that were able to
291 predict the intrinsic characteristics (i.e. pH, soluble solid content, titratable acidity) but that proved to
292 poorly estimate sensory parameters of table grape such as visual quality.

293 In addition, to average cross-validation classification accuracy on training and test sets, Table 2 and
294 Table 3 show the confusion matrices obtained by the classification model using automatically selected
295 features. This more detailed information can be useful to judge the kinds of errors made by the system
296 and their relevance to the specific application needs. Different errors can correspond to different costs
297 and this information can be used to judge the economic impact of errors and tune the classification
298 strategy according to the required economic risk.

299 The experiments showed that it is possible to use a CVS to non-destructively and contactless evaluate
300 the quality of table grapes by developing classification model that are specific for single cultivars. The
301 performance of the system on each cultivar does not depend on the storage temperature making it
302 practically useful in real context where the temperature can be confined into specific range but cannot
303 be kept constant **around a fixed point**.

304 Further experiments have been planned to try to understand the source of the different performances
305 on different cultivars. Globally, the system appears to be able to provide an effective answer to the
306 request of a non-destructive and contactless method to grade completely the production in a more
307 objective and reliable way with respect to human made visual evaluation. In addition, the system
308 compares favourably with costs and time required by the destructive analytical tests made in the
309 laboratory.

310 **4.0. Conclusions**

311 A Computer vision system for the non-destructive and contactless evaluation of quality of table grapes
312 has been presented. It has been verified on two table grape cultivars (**Italia and Victoria**) showing
313 good performance on the task of checking and detecting when the product reaches the QL 3, that
314 represents the limit of marketability and therefore require specific management actions to be assumed.

315 The Computer vision system uses image processing techniques to process and analyse colour images
316 and achieve the required classification. It also exploits a few machine learning methodologies to
317 simplify the configuration and tuning of the algorithms avoiding human intervention as much as
318 possible without performance loss. On the contrary, the experiments showed that automatic features

319 selection outperformed manually selected features. This assisted configuration makes easier to extend
320 its application to different situations along the supply chain and to different cultivars. The Computer
321 vision system represents a suitable tool to solve the request for a quality evaluation tool that can be
322 applied to the whole production and provide an objective answer with lower cost in terms of time and
323 money with respect to the destructive tests in laboratory.

324

325 **Acknowledgments**

326 The research leading to these results has received funding from Puglia Regional call ‘Avviso Aiuti a
327 Sostegno dei Cluster Tecnologici Regionali per l’Innovazione’. Continnova Project: Container
328 innovativo isothermico intermodale equipaggiato con atmosfera controllata per il trasporto di prodotti
329 ortofrutticoli freschi (cod.VFQA3D0). The authors thank Salvatore Cervellieri, Arturo Argentieri and
330 Michele Attolico for the technical support to the configuration of the experimental set-up and
331 Giacomo Suglia President of APEO (Associazione Produttori Esportatori Ortofrutticoli) for the kind
332 collaboration.

333

334 **References**

- 335 Amodio, M.L., Cabezas-Serrano, A.B., Peri, G., Colelli, G. 2011. Post-cutting quality changes of
336 fresh-cut artichokes treated with different anti-browning agents as evaluated by image analysis.
337 *Postharvest Biol. Technol.* 62, 213-220.
- 338 Amodio, M.L., Cabezas-Serrano, A.B., Rinaldi, R., Colelli, G. 2007. Implementation of rating scales
339 for visual quality evaluation of various vegetable crops, in: Kader, A.A., Cantwell, M. (Eds.),
340 *Produce Quality Rating Scales and Colour Charts*, Postharvest Horticulture Series No. 23.
341 University of California, Davis, CA-USA.
- 342 Aquino, A., Barrio, I., Diago, M., Millan, B., Tardaguila, J. 2018a. *vitisBerry: an Android-smartphone*
343 *application to early evaluate the number of grapevine berries by means of image analysis. Comput.*
344 *Electron. Agric.* 148, 19-28.
- 345 Aquino, A., Millan, B., Diago, M. P., Tardaguila, J. 2018b. Automated early yield prediction in
346 vineyards from on-the-go image acquisition. *Comput. Electron. Agric.*
347 <https://doi.org/10.1016/j.compag.2017.11.026>
- 348 Arias, R., Lee, T.C., Logendra, L. Janes, H. 2000. Correlation of lycopene measured by HPLC with
349 the L*, a*, b* colour readings of a hydroponic tomato and the relationship of maturity with colour
350 and lycopene content. *J. Agr. Food Chem.* 48, 1697-1702.
- 351 Bahar, A., Kaplunov, T., Alchanatis, V., Lichter, A. 2017. Evaluation of methods for determining
352 rachis browning in table grapes. *Postharvest Biol. Technol.* 134, 106-113.
- 353 Baiano, A., Terracone, C., Peri, G., Romaniello, R. 2012. Application of hyperspectral imaging for
354 prediction of physico-chemical and sensory characteristics of table grapes. *Comput. Electron.*
355 *Agric.* 87, 142-151.
- 356 Blasco, J., Munera, S., Aleixos, N., Cubero, S., Moltó, E. 2017. Machine Vision-Based Measurement
357 Systems for Fruit and Vegetable Quality Control in Postharvest, in: Hitzmann, B. (Eds),
358 *Measurement, Modeling and Automation in Advanced Food Processing. Advances in Biochemical*
359 *Engineering/Biotechnology.* Springer Berlin Heidelberg, Germany, 161, 71-92.

360 Cavallo, D.P., Cefola, M., Pace, B., Logrieco, A.F., Attolico, G. 2017. Contactless and non-
361 destructive chlorophyll content prediction by random forest regression: A case study on fresh-cut
362 rocket leaves. *Comput. Electron. Agric.* 140, 303-310.

363 Cavallo, D.P., Cefola, M., Pace, B., Logrieco, A.F., Attolico, G. 2018. Non-destructive automatic
364 quality evaluation of fresh-cut iceberg lettuce through packaging material. *J. Food Eng.* 223, 46-52.

365 Cefola, M., Damascelli, A., Lippolis, V., Cervellieri, S., Linsalata, V., Logrieco, A.F., Pace, B. 2018.
366 Relationships among volatile metabolites, quality and sensory parameters of 'Italia' table grapes
367 assessed during cold storage in low or high CO₂ modified atmospheres. *Postharvest Biol. Technol.*
368 142, 124-134.

369 ~~Costa, G., Noferini, M., Fiori, G., Torrigani, P. 2009. Use of Vis/NIR Spectroscopy to assess fruit
370 ripening stage and improve management in post-harvest chain. *Fresh Prod.* 1, 35-41.~~

371 Diago, M. P., Tardaguila, J., Aleixos, N., Millan, B., Prats-Montalban, J. M., Cubero, S., & Blasco, J.
372 (2015). Assessment of cluster yield components by image analysis. *J. Sci. Food Agric*, 95(6),
373 1274–1282. <https://doi.org/10.1002/jsfa.6819>

374 Lichter, A., 2016. Rachis browning in table grapes. *Aust. J. Grape Wine Res.* 22, 161-168.

375 Liu, Y., Pu, H., Sun, D.W. 2017. Hyperspectral imaging technique for evaluating food quality and
376 safety during various processes: A review of recent applications. *Trends Food Sci. Technol.* 69, 25-
377 35.

378 Nogales-Bueno, J., Hernández-Hierro, J. M., Rodríguez-Pulido, F. J., & Heredia, F. J. (2014).
379 Determination of technological maturity of grapes and total phenolic compounds of grape skins in
380 red and white cultivars during ripening by near infrared hyperspectral image: A preliminary
381 approach. *Food Chem*, 152, 586–591. <https://doi.org/10.1016/j.foodchem.2013.12.030>

382 OIV. (2008). Resolution VITI 1/2008: OIV standard on minimum maturity requirements for table
383 grapes.

384 Pace, B., Cavallo, D.P., Cefola, M., Attolico, G. 2017. Automatic identification of relevant colors in
385 non-destructive quality evaluation of fresh salad vegetables. *Int. J. Food Process. Technol.* 4, 1-5.

386 Pace, B., Cavallo, D.P., Cefola, M., Colella, R., Attolico, G. 2015. Adaptive self-configuring
387 computer vision system for quality evaluation of fresh-cut radicchio. *Innov. Food Sci. Emerg.*
388 *Technol.* 32, 200-207.

389 Pace, B., Cefola, M., Da Pelo, P., Renna, F., Attolico, G. 2014. Non-destructive evaluation of quality
390 and ammonia content in whole and fresh-cut lettuce by computer vision system. *Food Res. Int.* 64,
391 647-655.

392 Pace, B., Cefola, M., Renna, F., Attolico, G. 2011. Relationship between visual appearance and
393 browning as evaluated by image analysis and chemical traits in fresh-cut nectarines. *Postharvest*
394 *Biol. Technol.* 61(2), 178-183.

395 Patel, K.K., Kar, A., Jha, S.N., Khan, M.A. 2012. Machine vision system: a tool for quality inspection
396 of food and agricultural products. *J. Food Sci. Technol.* 49, 123-141.

397 Pothen, Z., Nuske, S. 2016. Automated assessment and mapping of grape quality through image-
398 based color analysis. *IFAC-PapersOnLine.* 49(16), 72-78.

399 Raban, E., Kaplunov, T., Zutahy, Y., Daus, A., Alchanatis, V., Ostrovsky, V., Lurie S., Lichter, A.
400 2013. Rachis browning in four table grape cultivars as affected by growth regulators or packaging.
401 *Postharvest Biol. Technol.* 84, 88–95. <https://doi.org/10.1016/j.postharvbio.2013.03.021>

402 Rahman, A., Hellicar, A. 2014. Identification of mature grape bunches using image processing and
403 computational intelligence methods. In *2014 IEEE Symposium on Computational Intelligence for*
404 *Multimedia, Signal and Vision Processing (CIMSIVP)* (pp. 1–6). IEEE.
405 <https://doi.org/10.1109/CIMSIVP.2014.7013272>

406 Rodriguez-Pulido, F.J., Gómez-Robledo, L., Melgosa, M., Gordillo, B., Gonzàles-Miret, M.L.,
407 Heredia, F.J. 2012. Ripeness estimation of grape berries and seeds by image analysis. *Comput.*
408 *Electron. Agric.* 82, 128-133.

409 Sollazzo, M., Baccelloni, S., D’Onofrio, C., Bellincontro, A. 2018. Combining color chart,
410 colorimetric measurement and chemical compounds for postharvest quality of white wine grapes.
411 *J. Sci. Food Agric.* <https://doi.org/10.1002/jsfa.8864>.

CV ITALIA

CV VICTORIA

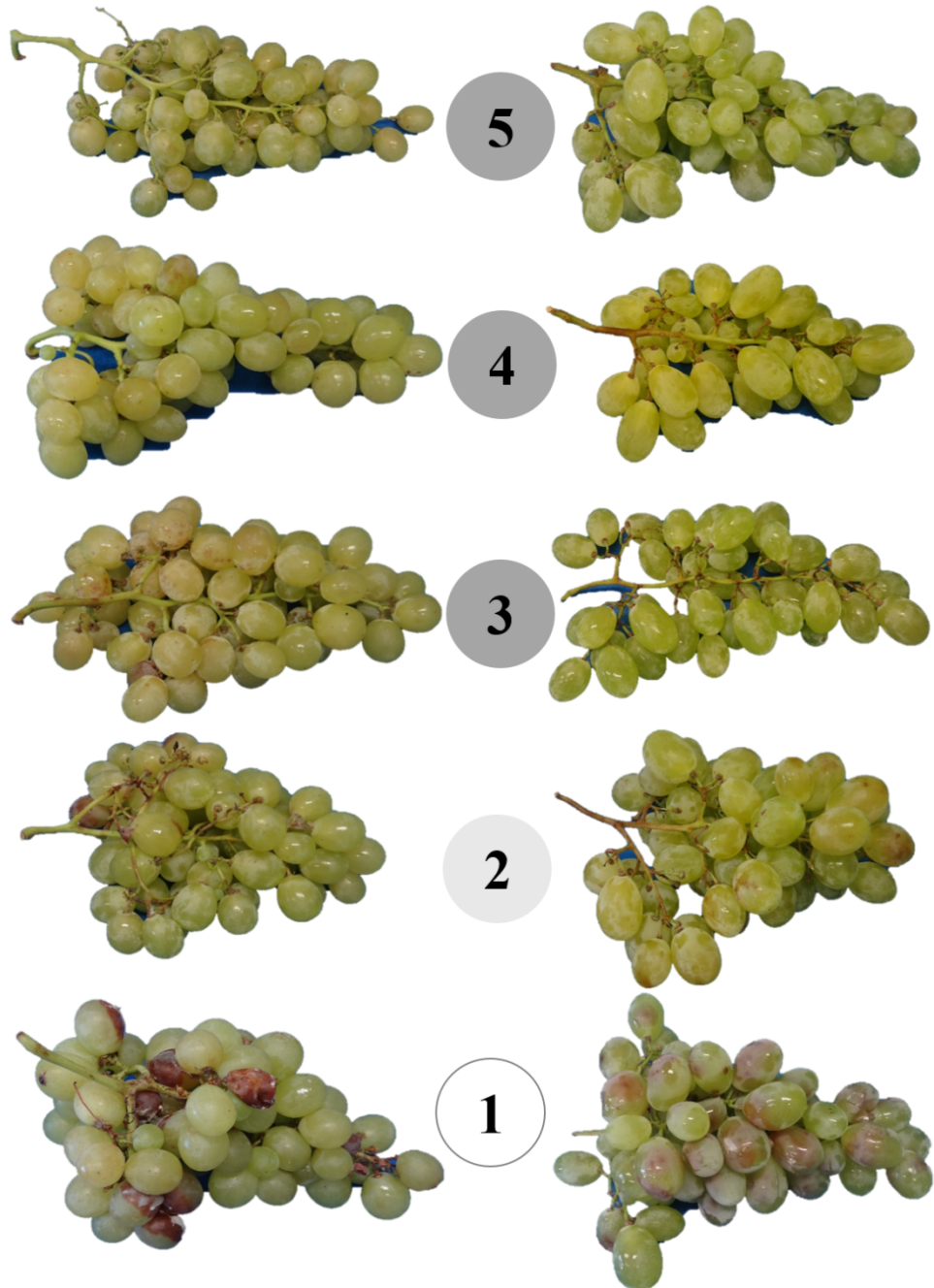


Figure 1. Quality level rating scale for table grapes of cultivars Italia and **Victoria**.

5= very good (rachis green, firm berries, no signs of decay), 4 = good (rachis green with slight symptom of dehydration, firm berries), 3 = limit of acceptability or marketability (rachis moderately browned, firm berries slightly brown), 2 = poor (evident signs of browning of rachis, loss of firmness of berries), and 1 = very poor (unacceptable quality due to decay).

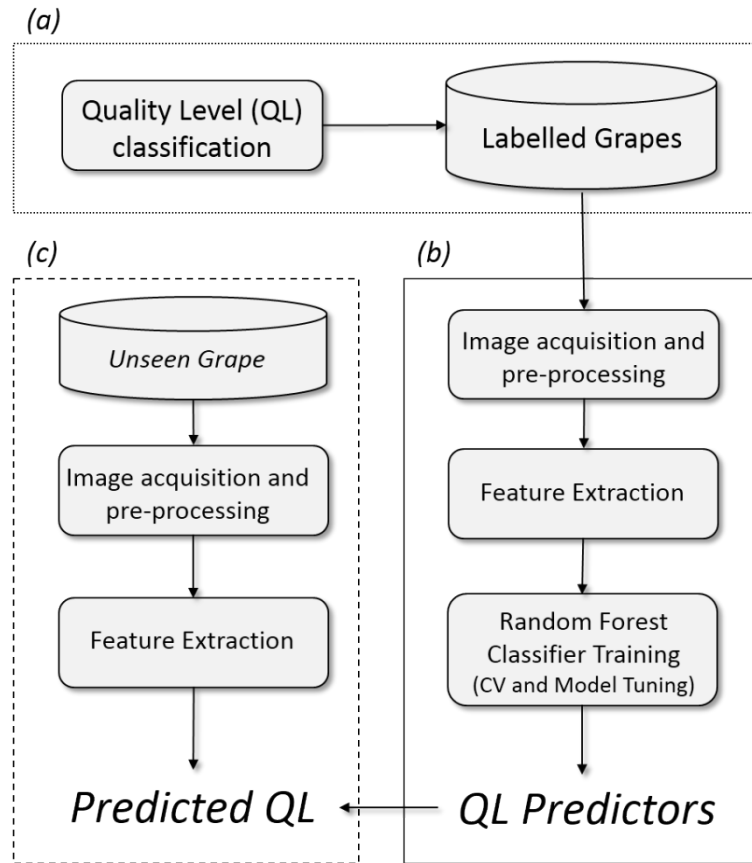


Figure 2. The three phases of the proposed approach: (a) all the table grapes were classified by experts according to 5 quality level (QL) where the fresh product corresponds to quality 5 and the worst product (waste) to quality 1; (b) all the classified table grapes were acquired and processed by the CVS, 14 numerical features were identified and an ensemble Random Forest classifier was trained, tuned and tested using the training set; (c) the validated model was used to classify unseen table grapes.

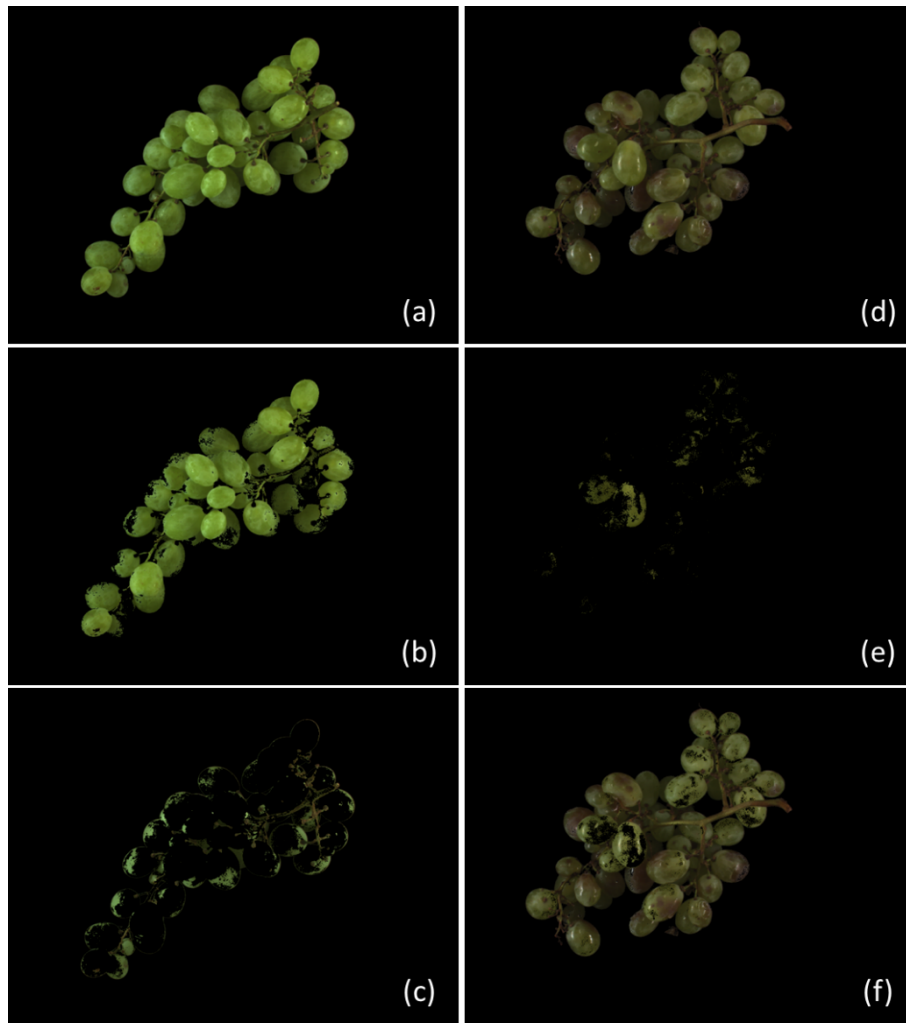


Figure 3. An example of centroid-based segmentation of images of table grapes (cv Italia) belonging to QL 5 (a, b, c) and QL 1 (d, e, f). A hierarchical clustering unsupervised technique was applied on a set of pixels representing the whole dataset. Then, each image was segmented by these centers and the number of pixels (for each segment) was used to identify percentage-based features.

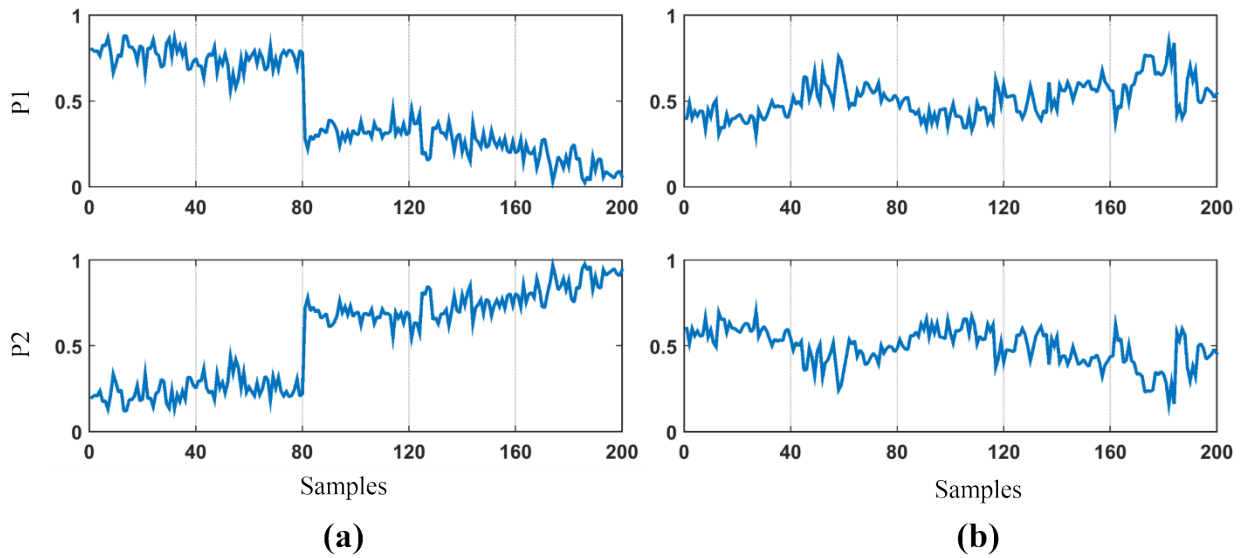


Figure 4. These graphs show on the y-axis the percentages of color 1 (P1) and of color 2 (P2) for table grapes of cultivar Italia (a) and Victoria (b) stored at 10°. The digital images of bunches are ordered along the x-axis from left to right from the highest quality (QL5) to the lowest (QL1). **QL 5 goes from 1 to 40, QL 4 from 41 to 80, QL3 from 81 to 120, QL2 from 121 to 160, QL1 from 161 to 200.** Features P1 and P2 are much more significant in the case of the cultivar Italia. The same trends were observed in the samples stored at 5°.

Table 1. Cross-Validation classification accuracy for the cultivar Italia and Victoria obtained using the Random Forest model verified on 3 different classification tasks: 5 classes, 3 classes and 2 classes. Moreover, its performance has been checked on both manually selected features (“Mean(L*, a*, b*), p1, p2”) and automatically selected features. The results assess the efficacy of our approach using a self-configuring and mostly automatic CVS.

Feature Selection	Classification task	Cross-Validation classification accuracy	
		cv Italia	cv Victoria
Mean(L*, a*, b*), p1, p2	QL5 vs QL4 vs QL3 vs QL2 vs QL1	0.72	0.6
Automatically selected features	QL5 vs QL4 vs QL3 vs QL2 vs QL1	0.74	0.71
Mean(L*, a*, b*), p1, p2	{QL5, QL4} vs QL3 vs {QL2, QL1}	0.91	0.78
Automatically selected features	{QL5, QL4} vs QL3 vs {QL2, QL1}	0.94	0.83
Mean(L*, a*, b*), p1, p2	{QL5, QL4} vs {QL3, QL2, QL1}	1.0	0.92
Automatically selected features	{QL5, QL4} vs {QL3, QL2, QL1}	1.0	0.92

Table 2. Further data about the performance of the Random Forest model (with automatic feature selection) on the cultivar Italia for all the three considered classification tasks: the **average** Cross-Validation (CV) Accuracy observed **on both the training and test sets** and the confusion matrix **on the test set**. In the confusion matrix, the columns represent the classification made by the CVS while the rows express the true class of the samples. Therefore, the number of samples belonging to each class is given by the sum of the values on each row.

Classification task	CV classification Accuracy		Confusion Matrix (test)						
	Training	Test	QL1	QL2	QL3	QL4	QL5		
QL5 vs QL4 vs QL3 vs QL2 vs QL1	0.99	0.75	49	24	7	0	0	QL1	
			15	51	14	0	0	QL2	
			3	9	68	0	0	QL3	
			0	0	0	63	17	QL4	
			0	0	0	10	70	QL5	
{QL5, QL4} vs QL3 vs {QL2, QL1}	0.99	0.94	151		9		0	QL1	
			16		64		0	QL2	
			0		0		160	QL4	
								160	QL5
{QL5, QL4} vs {QL3, QL2, QL1}	1	1		240			0	QL1	
									QL2
									QL3
					0			160	QL4
									160

Table 3. Further data about the performance of the Random Forest model (with automatic feature selection) on the cultivar Victoria for all the three considered classification tasks: the average Cross-Validation (CV) Accuracy observed on both the training and test sets and the confusion matrix on the test set. In the confusion matrix, the columns represent the classification made by the CVS while the rows express the true class of the digital images acquired on table grape bunches. Therefore, the number of images belonging to each class is given by the sum of the values on each row.

Classification task	CV		Confusion Matrix (test)						
	Classification Accuracy		QL1	QL2	QL3	QL4	QL5		
	Training	Test							
QL5 vs QL4 vs QL3 vs QL2 vs QL1	0.99	0.71	72	5	2	1	0	QL1	
			9	57	12	2	0	QL2	
			0	17	45	9	9	QL3	
			0	3	11	46	20	QL4	
			0	0	4	11	65	QL5	
{QL5, QL4} vs QL3 vs {QL2, QL1}	0.99	0.83	141		14		5	QL1	
			20		44		16	QL2	
			2		13		145	QL3	
								QL4	
{QL5, QL4} vs {QL3, QL2, QL1}	1	0.92			223		17	QL1	
								QL2	
								QL3	
					17			143	QL4
									QL5